Reconstructed Droop Control for Peer Current Sharing of Battery Storage in DC Microgrids

Fulong Li
School of Mechanical, Electrical and Manufacturing Engineering
Loughborough University
Loughborough, United Kingdom
Email: f.li@lboro.ac.uk

Haoge Xu
School of Mechanical, Electrical and Manufacturing Engineering
Loughborough University
Loughborough, United Kingdom
Email: h.xu2@lboro.ac.uk

Zhengyu Lin
School of Mechanical, Electrical and Manufacturing Engineering
Loughborough University
Loughborough, United Kingdom
Email: z.lin@lboro.ac.uk

***Abstract*—Droop control has been widely applied in DC microgrids for regulating the power sharing of battery storage. However, conventional droop control needs to select appreciate droop coefficients and large droop coefficients could have the potential to change the system quiescent operating point, thus causing instability. To solve such concern, this paper proposes a novel droop control realization with a natural droop coefficient. A reconstructed control block is used to achieve this purpose. The reconstructed control block also generates a controllable variable for integrating with hierarchical control scheme. Besides, this variable enhances the stability performance of converter due to variable load-adjusted bandwidth of controller. Numerical analysis is provided to visually inspect to the relationship between the bandwidth of controller and load power. A Matlab/simulink model is used to validate this novel reconstructed droop control.**

***Index Terms*—battery storage, controller design, current sharing, droop control, DC microgrids.**

I. Introduction

DC microgrids [1] have the potential to be the future power distribution structure due to its high integration with renewable energy sources (RES), such as photovoltaic (PV), wind turbine (WT) and fuel cell, etc. An example DC microgrid is shown in Fig. 1. It mainly has three parts, which are interface converters, power generations sources or energy storage, and common DC bus, respectively. The control of the interface converters is vital for efficient and reliable operation of the entire DC microgrid system.

Droop control has been widely applied [2]–[4] in the DC microgrids because of its easy implementation and natural power sharing in a distributed manner between distributed energy sources. Current sharing function of droop control provides an effective means for the power regulation of battery storage [3] in DC microgrids. Different droop coefficients combination can be adopted to regulate the battery distribution power [4]. Besides, the virtual resistance can be adjusted by the battery state of charge (SoC) so that the power regulation between battery storage can be optimized through SoC. A double-quadrant SoC based droop control method to regulate battery power in the case of overuse is proposed in paper [5]. Other related SoC-based droop control methods have been used in papers [6]–[12] for coordinating multiple battery banks [6]–[8], multiple supercapacitors [9], [10], and hybrid energy storage [11], [12]. From previous research, it can be found that the power sharing between energy storage is still based on the conventional droop control methods. The change on droop coefficient is a popular means to coordinate those energy storage.

This work has received funding from the U.K. EPSRC UKRI Innovation Fellowship scheme under grant No. EP/S001662/2, and the European Union's Horizon 2020 research and innovation programme under grant agreement No.734796.

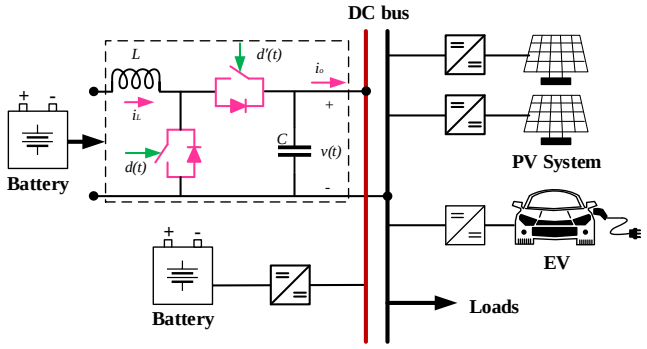

Fig. 1. An example DC microgrid configuration with multiple battery storage.

It is known that conventional droop control introduces virtual resistance (or droop coefficient) multiplied by output current to modify the voltage reference. When the load power increases, a significant voltage drop will be generated. The selection of virtual resistance limits this maximum allowed voltage drop, which means large droop coefficient may destabilize the system [13]. The large droop coefficient is yet important for improving current sharing accuracy. To deal with significant voltage drop, a secondary control is normally introduced. A low bandwidth communication (LBC) to realize the DC bus voltage restoration is proposed in [13], by adding an additional value to modify the voltage reference. In fact, the reason of such issue is that introduced virtual resistance lies outside of the closed voltage loop and the voltage loop control will not able to adaptively change control bandwidth when such voltage drop alters the previous quiescent operating point. Therefore, previous designed voltage compensator is

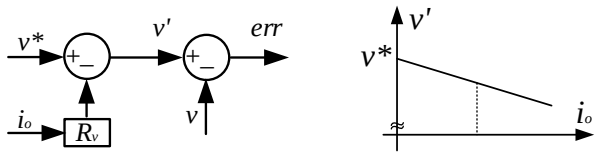

(a) Conventional droop control blocks (b) a typical droop curve

Fig. 2. Control block and VI curve of conventional droop control.

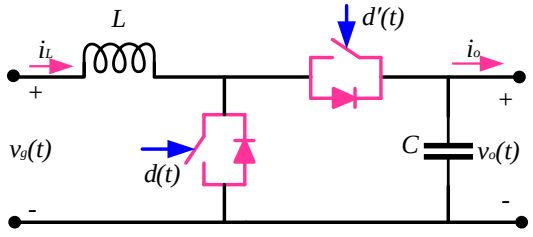

Fig. 3. Boost converter circuit.

no longer able to effectively regulate the output voltage. The consequence is the instability of entire system.

Driven by the above concern, this paper proposes a method to automatically stabilize the system by adapting the bandwidth of closed voltage loop when load changes. To achieve that, we reconstruct the droop control and make droop coefficient participate in the voltage closed loop control. Compared with conventional droop control methods, the reconstructed droop control has two improvements:

- Introduce a deterministic droop coefficient (can be modified certainly);
- Adaptively decrease the voltage closed loop bandwidth when the load increases such that stability operation can be promised.

The rest of this paper is organized as follows: Section II introduces the basic concept of droop control and identify of problem of conventional droop control in boost converters. Section III explains the construction process of proposed droop control. Section IV uses a Matlab/Simulink model to validate the proposed novel droop control, and a comparison with conventional droop control is provided. Finally, the concluding remarks are made in the Section V.

II. Droop Control and Problem Statement

To achieve conventional droop control, a virtual resistance is introduced. As for an ideal tightly regulated interface converter, the output impedance over low frequency range approximate to be zero. This means that when there are two distributed energy sources are connected in parallel, it will generate a large circulating current between them even if a tiny output voltage difference exists. Therefore, virtual resistance is introduced to avoid this situation.

This virtual resistance is multiplied by the output current to form a new voltage reference for the primary double loop control, which is shown in Fig. 2(a). The terminal voltage will have voltage droop when the load increases, which is shown in Fig. 2(b). This relationship can be written as equation (1), which has already been discussed in many paper [2]–[4].

$$v' = v^* - i_o R_v \tag{1}$$

where v' is the real voltage reference; v^* is the nominal voltage; R_v is the virtual resistance; i_o is the output current.

However, droop control has two main drawbacks. First, the voltage droop caused by the droop control is not desired in many applications need a constant DC bus voltage. Second, the combination of the droop coefficient affects the accuracy of the power/current sharing between energy storage and may be affected by the line resistance. Fortunately, those issues can be solved by the secondary control.

It can be seen from the equation (1) that the output voltage of conventional droop control will decrease when the load power/current increase. This may lead to the primary current and voltage compensator no longer suitable for current working conditions, or instability in other words. The reason lies that the previous voltage compensator is designed through voltage reference v^* and introduced droop control makes the real voltage reference drop below this value. Even though the secondary control is able to recover the bus voltage droop as aforementioned, the limited bandwidth of primary controller is unable to handle this voltage droop. Therefore, it is necessary to make the primary controller to relax the bandwidth when the load changes.

III. Reconstruction of Droop Control

A. Modelling and Analysis

Boost converter is used in this paper and the circuit is shown in Fig. 3. Through analyzing the power switch ON and OFF state, average state equations can be written as equation (2) and (3).

$$L\frac{di_L(t)}{dt} = v_g(t) - d'(t)v(t) \tag{2}$$

$$C\frac{dv(t)}{dt} = d'(t)i_L(t) - i_o(t) \tag{3}$$

where $v_g(t)$ is the input voltage of source, $i_L(t)$ is the inductor current, $v(t)$ is the terminal voltage, $i_o(t)$ is the output current, $d'(t)$ is equal to $1-d(t)$ and $d(t)$ is the duty cycle of the PWM signal.

Transfer above equations into s domain,

$$i_L(s) = \frac{v_g(s) - d'(s)v(s)}{sL} \tag{4}$$

$$v(s) = \frac{d'(s)i_L(s) - i_o(s)}{sC} \tag{5}$$

Apply small ac variations and assume the input voltage is constant, the following equations can be attained.

$$\Delta i_L(s) = \frac{\Delta d(s)V - D'\Delta v(s)}{sL} \tag{6}$$

$$\Delta v(s) = \frac{-\Delta d(s)I_L + D'\Delta i_L(s) - \Delta i_o(s)}{sC} \tag{7}$$

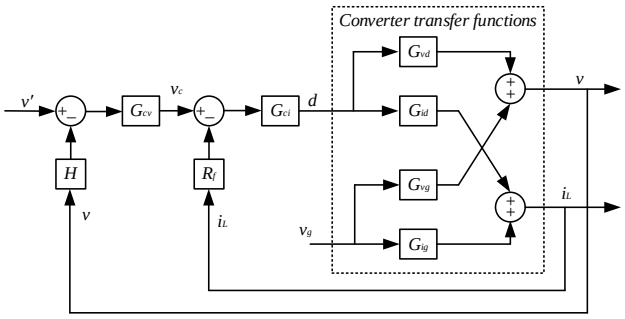

Fig. 4. Boost converter transfer function map.

Several typical transfer functions for the boost converter are listed below from equation (8) to equation (11).

$$G_{vd}(s) = \frac{V}{D'}\frac{1 - s\frac{L}{D'^2R}}{den(s)} \tag{8}$$

$$G_{id}(s) = \frac{2V}{D'^2R}\frac{1 + s\frac{RC}{2}}{den(s)} \tag{9}$$

$$G_{vg}(s) = \frac{1}{D'}\frac{1}{den(s)} \tag{10}$$

$$G_{ig}(s) = \frac{1}{D'^2R}\frac{1 + sRC}{den(s)} \tag{11}$$

where $den(s) = 1 + s\frac{L}{D'^2R} + s^2\frac{LC}{D'^2}$.

The transfer function map of a boost converter is shown in Fig. 4, the outer loop plant is the transfer function of inductor current reference to output voltage [14], as is shown in equation (12).

$$G_{vc} = \frac{\Delta v}{\Delta v_c} = \frac{\Delta v}{\Delta d}\cdot\frac{\Delta d}{\Delta v_c} \tag{12}$$

Δv_c approximately equals to the inductor current multiplying the current sampling resistor R_f, which is because the purpose of the controller is trying to tune the value of inductor current to follow the value of Δv_c. Therefore,

$$\Delta v_c = \Delta i_L^* R_f \approx R_f \Delta i_L \tag{13}$$

Replace Δv_c in the equation (12) with the equation (13), then the outer loop plant can be obtained below,

$$G_{vc} = \frac{\Delta v}{\Delta v_c} \approx \frac{\Delta v}{\Delta d}\cdot\frac{\Delta d}{R_f\Delta i_L} = \frac{1}{R_f}\cdot\frac{G_{vd}}{G_{id}} \tag{14}$$

Replace the transfer functions G_{vd} and G_{id} in the equation (14) with equation (8) and (9), the outer loop control plant can be written as equation (15).

$$G_{vc} \approx \frac{1}{R_f}\cdot\frac{G_{vd}}{G_{id}} = \frac{D'R}{2R_f}\cdot\frac{1 - s\frac{L}{D'^2R}}{1 + s\frac{RC}{2}} \tag{15}$$

It can be seen from the equation (15) that the output voltage plant is a first order system, which is easier to design a compensator compared with directly controlling the voltage plant G_{vd} in a single loop control.

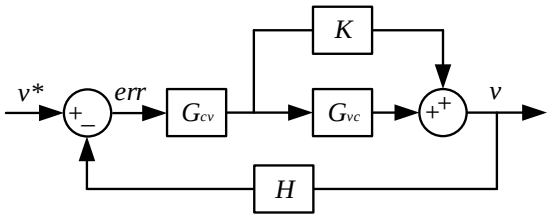

Fig. 5. Introducing a feedforward path in the outer voltage loop [15].

B. Proposed Novel Droop Control

Introducing a feedforward control path as the paper [15] described, which is shown in Fig. 5, the stability performance of boost converter will be improved. The reason of adding this control path is that the introduced feedforward path alters the DC components with additional gain K meanwhile compensate the non-minimum phase as is shown in the equation (15). The new output voltage loop control plant then becomes,

$$G'_{vc} = K + G_{vc} \tag{16}$$

where G'_{vc} is the new control plant compensated by feedforward path shown in the Fig. 5.

Combine equation (15) and (16), the low and high frequency asymptotic of this new control plant can be written as:

$$s \to 0, \quad G'_{vc} \to \frac{D'R}{2R_f} + K \tag{17}$$

$$s \to +\infty, \quad G'_{vc} \to K - \frac{L}{R_f D'RC} \tag{18}$$

Normally, the value of K is designed large enough to ensure G'_{vc} is always large than zero as analyzed in the paper [15]. Notice that this negative value is relative to the load R; and this parameter can be converted into output voltage divided by output current. Therefore, a new feedforward gain K' is defined,

$$K' = \frac{L}{R_f V_g C} \tag{19}$$

It can be seen that the new defined K' is related to the converter component values only. Therefore, when the voltage control loop introduces the output current, then the following equation can be satisfied.

$$K = i_o K' = i_o\frac{L}{R_f V_g C} = \frac{VL}{RR_f V_g C} = \frac{L}{R_f D'RC} \tag{20}$$

The control block of novel droop control is finished. From equation (17), the low frequency gain is affected by this additional K. Therefore, the manipulation over the mid-high frequency as discussed from equation (18) to equation (20) can directly work on the formation of this voltage droop over low frequency.

The modified control path with introducing output current, from above analysis, is shown in Fig. 6. The current and

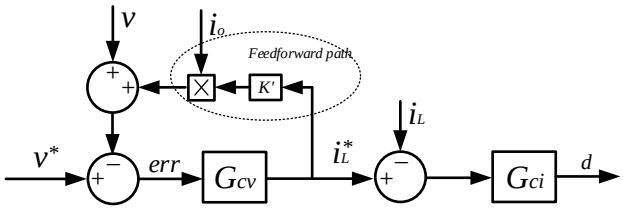

Fig. 6. Control block of proposed droop control.

voltage compensator shown in Fig. 6 are designed to be typical PI controllers and written as:

$$G_{ci}(s) = G_{im}\left(1 + \frac{2\pi f_{zi}}{s}\right) \tag{21}$$

$$G_{cv}(s) = G_{vm}\left(1 + \frac{2\pi f_{zv}}{s}\right) \tag{22}$$

where $G_{ci}(s)$ is the inner current loop compensator; G_{im} is current compensator gain; $G_{cv}(s)$ is outer voltage loop compensator; G_{vm} is voltage compensator gain.

C. Output Impedance Discussions

The output impedance of conventional droop control will approximate the introduced virtual resistance R_v, which can be written in equation (23).

$$s \to 0, Y_T^D \to \frac{1}{R_v} \Rightarrow Z_T^D \to R_v \tag{23}$$

where Y_T^D is output admittance of boost converter and Z_T^D is output impedance of boost converter.

A feedforward path is introduced to the output loop control plant. Within this feedforward path, a natural low frequency impedance forms, equivalent to the conventional droop coefficient, and closed voltage loop bandwidth will adaptively change according to the load power as the output current is introduced in this path. The output impedance of proposed drop control can be written as:

$$Z_T^D \to K' I_L = \frac{K' I_o}{D'} \tag{24}$$

It can be seen from equation (24) that the output impedance of proposed control is determined by the output power and converter itself parameters. From this point, the output current sharing can also be influenced by adding other controllable variable to the gain K', such as SoC, for battery storage applications.

IV. Simulation Validations

A. Numerical Analysis

The numerical analysis is based on the parameters discussed above and values listed in the Table. I. The relationship of bandwidth of outer voltage loop and load power is shown in Fig. 7. From this figure, the bandwidth adjustment and load power is almost linearly fitted. When the load increases, the bandwidth automatically reduces to ensure system stability. This exactly matches the design expectations.

TABLE I
Parameters and Values

Parameter	*Values*	*Meaning*
L	$240\mu H$	Inductor
C	$470\mu F$	Capacitor
R	$2-50\Omega$	Load resistor
V_g	$25V$	Input source voltage
C	$470\mu F$	Output capacitor
v^*	$50V$	Reference voltage/nominal voltage
f_s	$25kHz$	Switching frequency
R_v	$0.5-5.0$	Virtual resistance
f_{zi}	$1kHz$	Inner loop current controller zero frequency
f_{zv}	$250Hz$	Outer loop voltage controller zero frequency

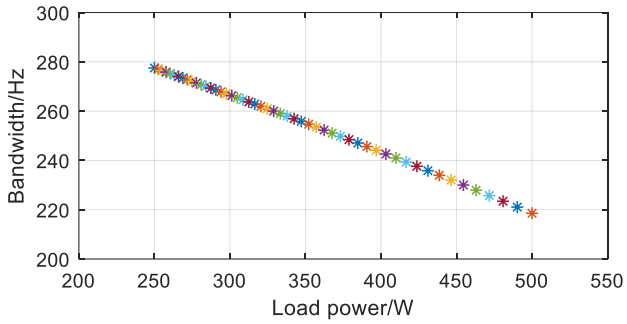

Fig. 7. Relationship of bandwidth of outer voltage loop and load power.

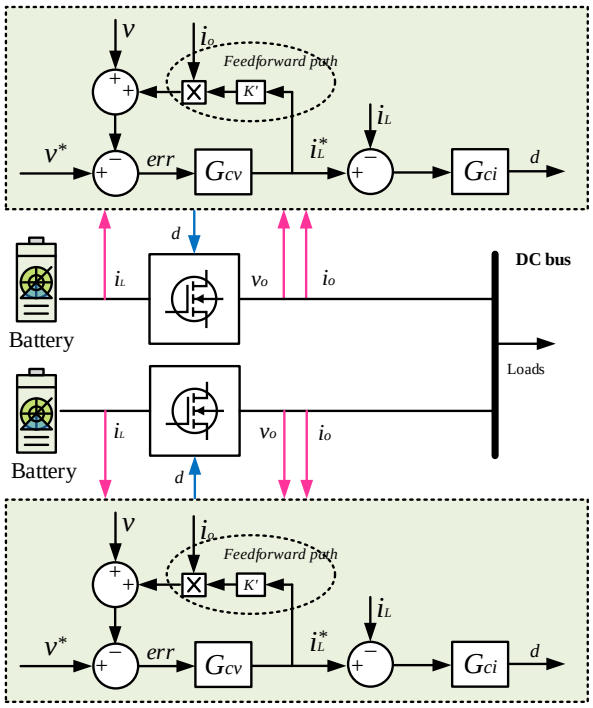

Fig. 8. Simulation constructions.

B. Simulation Results

The configurations of the simulink model is shown in Fig. 8 where two battery storage connected in parallel via boost converters. This simulation model is used to validate the

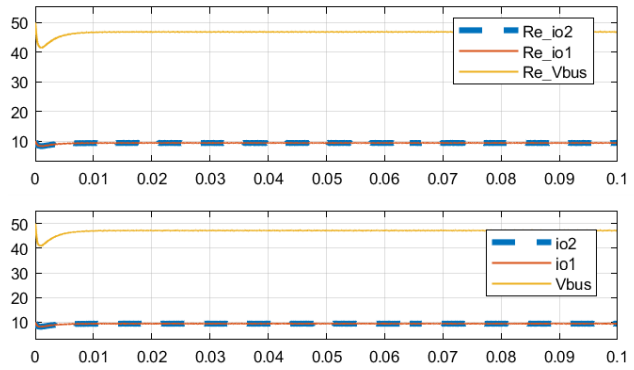

Fig. 9. Simulation validation without heavy load stepping.

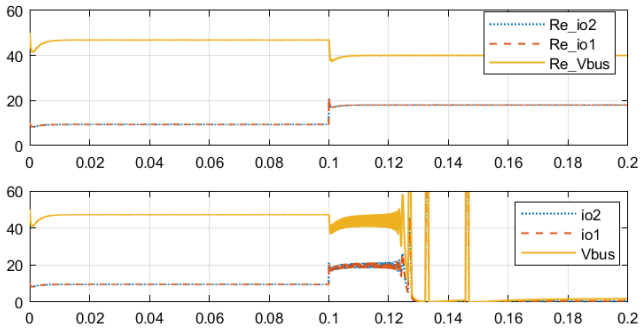

Fig. 10. Simulation validation with heavy load stepping.

proposed reconstructed droop control. A comparative study with conventional droop control is made.

Firstly, when the system is operated in the normal conditions without heavy load stepping, both conventional droop control and proposed droop control can manage the system very well. The simulation result is shown in Fig. 9. The top part of the figure shows the results of reconstructed droop control and the bottom part shows the results of conventional droop control. The nominated voltage reference v^* is set to be 50V, and a voltage droop can be observed in the figure. An average current sharing is used in this case. It can be seen that the current between two battery storage is shared equally as expected.

Secondly, when the system encounter a heavy load stepping, the performance of proposed droop control is better than the conventional droop control. The simulation result is shown in the Fig. 10, the heavy load steps at 0.1s. Again, the top part of the figure shows the results of reconstructed droop control and the bottom part shows the results of conventional droop control. The reconstructed droop control can manage the large voltage drop caused by the load stepping very well, which meets the theoretical prediction. However, the conventional droop control can not deal with this issue as analyzed, and the system becomes unstable eventually.

V. Conclusions

This paper proposed a novel droop control method for DC microgrid systems. Compared with conventional droop control methods, the proposed method has natural droop characteristics, there is thus no need to introduce virtual resistance. Besides, the proposed droop control method can self-adaptively tuning the controller bandwidth according to the loads variation, which gains more flexibility and reliability for DC microgrid operations. The reconstruction of droop control blocks is required and explained in detail in this paper. Finally, the simulation results prove the effectiveness of proposed novel droop control method.

References

[1] R. H. Lasseter, "Microgrids," in *002 IEEE Power Engineering Society Winter Meeting. Conference Proceedings (Cat. No.02CH37309)*, vol. 1, 1998, pp. 305–30 866 vol.1.

[2] F. Li, Z. Lin, Z. Qian, J. Wu, and W. Jiang, "A dual-window dc bus interacting method for dc microgrids hierarchical control scheme," *IEEE Transactions on Sustainable Energy*, vol. 11, no. 2, pp. 652–661, 2020.

[3] F. Li, Z. Lin, Z. Qian, and J. Wu, "Active dc bus signaling control method for coordinating multiple energy storage devices in dc microgrid," in *2017 IEEE Second International Conference on DC Microgrids (ICDCM)*, 2017, pp. 221–226.

[4] S. Augustine, M. K. Mishra, and N. Lakshminarasamma, "Adaptive droop control strategy for load sharing and circulating current minimization in low-voltage standalone dc microgrid," *IEEE Transactions on Sustainable Energy*, vol. 6, no. 1, pp. 132–141, 2015.

[5] X. Lu, K. Sun, J. M. Guerrero, J. C. Vasquez, and L. Huang, "Double-quadrant state-of-charge-based droop control method for distributed energy storage systems in autonomous dc microgrids," *IEEE Transactions on Smart Grid*, vol. 6, no. 1, pp. 147–157, 2015.

[6] T. Dragičević, J. M. Guerrero, J. C. Vasquez, and D. Škrlec, "Supervisory control of an adaptive-droop regulated dc microgrid with battery management capability," *IEEE Transactions on Power Electronics*, vol. 29, no. 2, pp. 695–706, 2014.

[7] N. L. Diaz, T. Dragičević, J. C. Vasquez, and J. M. Guerrero, "Intelligent distributed generation and storage units for dc microgrids—a new concept on cooperative control without communications beyond droop control," *IEEE Transactions on Smart Grid*, vol. 5, no. 5, pp. 2476–2485, 2014.

[8] X. Lu, K. Sun, J. M. Guerrero, J. C. Vasquez, and L. Huang, "State-of-charge balance using adaptive droop control for distributed energy storage systems in dc microgrid applications," *IEEE Transactions on Industrial Electronics*, vol. 61, no. 6, pp. 2804–2815, 2014.

[9] Y. Zhang and Y. Wei Li, "Energy management strategy for supercapacitor in droop-controlled dc microgrid using virtual impedance," *IEEE Transactions on Power Electronics*, vol. 32, no. 4, pp. 2704–2716, 2017.

[10] X. Zhao, Y. W. Li, H. Tian, and X. Wu, "Energy management strategy of multiple supercapacitors in a dc microgrid using adaptive virtual impedance," *IEEE Journal of Emerging and Selected Topics in Power Electronics*, vol. 4, no. 4, pp. 1174–1185, 2016.

[11] S. K. Kollimalla, M. K. Mishra, A. Ukil, and H. B. Gooi, "Dc grid voltage regulation using new hess control strategy," *IEEE Transactions on Sustainable Energy*, vol. 8, no. 2, pp. 772–781, 2017.

[12] Q. Xu, J. Xiao, P. Wang, X. Pan, and C. Wen, "A decentralized control strategy for autonomous transient power sharing and state-of-charge recovery in hybrid energy storage systems," *IEEE Transactions on Sustainable Energy*, vol. 8, no. 4, pp. 1443–1452, 2017.

[13] X. Lu, J. M. Guerrero, K. Sun, and J. C. Vasquez, "An improved droop control method for dc microgrids based on low bandwidth communication with dc bus voltage restoration and enhanced current sharing accuracy," *IEEE Transactions on Power Electronics*, vol. 29, no. 4, pp. 1800–1812, 2014.

[14] R. W. Erickson and D. Maksimović, *Fundamentals of Power Electronics*, 2nd ed. Boston, MA: Springer US, 2001, ch. 12, pp. 439–487.

[15] F. Li and Z. Lin, "Novel passive controller design for enhancing boost converter stability in dc microgrid applications," *IEEE Journal of Emerging and Selected Topics in Power Electronics*, pp. 1–1, 2021.